Biogeosciences Discuss., 7, 8177–8214, 2010
www.biogeosciences-discuss.net/7/8177/2010/
doi:10.5194/bgd-7-8177-2010

Biogeosciences Discussions

Impact of ocean acidification and elevated temperatures on early juveniles of the polar shelled pteropod *Limacina helicina*: mortality, shell degradation, and shell growth

S. Lischka, J. Büdenbender, T. Boxhammer, and U. Riebesell

Leibniz Institute of Marine Sciences (IFM-GEOMAR), Kiel, Germany

Received: 27 October 2010 – Accepted: 27 October 2010 – Published: 5 November 2010

Correspondence to: S. Lischka (slischka@ifm-geomar.de)

Published by Copernicus Publications on behalf of the European Geosciences Union.

Abstract

Due to their aragonitic shell thecosome pteropods may be particularly vulnerable to ocean acidification driven by anthropogenic CO_2 emissions. This applies specifically to species inhabiting Arctic surface waters that are projected to become locally undersaturated with respect to aragonite as early as 2016. This study investigated the effects of rising pCO_2 partial pressures and elevated temperature on pre-winter juveniles of the polar pteropod *Limacina helicina*. After a 29 days experiment in September/October 2009 at three different temperatures and under pCO_2 scenarios projected for this century, mortality, shell degradation, shell diameter and shell increment were investigated. Temperature and pCO_2 had a significant effect on mortality, but temperature was the overriding factor. Shell diameter, shell increment and shell degradation were significantly impacted by pCO_2 but not by temperature. Mortality was 46% higher at 8 °C compared to 3 °C (in situ), and 14% higher at 1100 µatm CO_2 as compared to 230 µatm CO_2. Shell diameter and increment were reduced by 10% and 12% at 1100 µatm CO_2 as compared to 230 µatm CO_2, respectively, and shell degradation was 41% higher at elevated compared to ambient pCO_2 partial pressures. We conclude that pre-winter juveniles will be negatively affected by both rising temperature and pCO_2 which may result in a possible abundance decline of the overwintering population, the basis for next year's reproduction.

1 Introduction

Anthropogenic CO_2 emissions affect the seawater carbonate chemistry and cause a decrease of seawater pH (termed ocean acidification) and carbonate ions in the worlds' oceans, thereby also diminishing the saturation state of seawater with respect to calcite and aragonite. This effect is strongest in high-latitude surface waters, which are also experiencing the steepest increase in surface ocean temperature (Orr et al., 2005;

BGD
7, 8177–8214, 2010

Steinacher et al., 2009). Due to increasing CO_2 emissions since the industrial revolution, global surface temperatures rose by 0.76 °C and global seawater pH decreased by 0.1 unit (IPCC 2007).

Calcite and aragonite are two common types of calcium carbonate secreted by marine organisms. Surface waters in the Arctic are projected to become locally undersaturated (and even more widespread as atmospheric CO_2 continues to grow) with respect to aragonite within a decade and this will first occur especially in surface waters during winter (Steinacher et al., 2009).

Changes of the carbonate chemistry can have severe consequences for marine organisms, particularly to those that build skeletons, shells, and tests of biogenic calcium carbonate. For instance, reduced calcification rates in corals, coralline macroalgae, coccolithophorids, bivalves, and echinoderms have been reported during the last years as a consequence of rising CO_2 partial pressures (e.g. Riebesell et al., 2000; Gazeau et al., 2007; Fabry et al., 2008). On the contrary, a recent study by Gutowska et al. (2010) revealed increased calcification in the cuttlebone of the cephalopod *Sepia officinalis* during exposure to elevated CO_2 partial pressures. Hence, organisms' response to carbonate system variations is diverse.

A widely held view, as articulated by Wilson (1973), has been that "*living things during early developmental stages are more sensitive than at any other time in their life cycle to adverse influences in the environment*". Also with respect to ocean acidification, several studies corroborate this view in that early developmental and reproductive stages of calcifiers are the most vulnerable stages within a life cycle (e.g. Kurihara et al., 2007; Kurihara 2008; Clark et al., 2009; Comeau at al., 2010a). These authors report for example on retarded larval development, reduced shell mineralization/calcification, increased mortality and degradation of larval skeleton in sea urchin and pteropod larvae, respectively. Acting on early developmental and reproductive stages, ocean acidification can have direct impact on population size and reduce fitness and increase mortality of the offspring, respectively (Kurihara, 2008). Thus it can have the capacity to change species distributions and abundances that could propagate

BGD
7, 8177–8214, 2010

through multiple trophic levels of the marine food web (Guinotte and Fabry, 2008).

Thecosome pteropods are widely distributed small-sized holoplanktonic marine mollusks. While their species diversity is high in tropical regions, only two epipelagic species, both of the genus *Limacina*, occur in temperate areas of the North Atlantic and in Arctic regions (van der Spoel, 1967). In northern and polar regions, pteropods can dominate zooplankton communities at times and are key species in epipelagic food webs both as consumers of and prey for various marine organisms, including commercially important fish, seabirds and baleen whales (Gilmer and Harbison, 1991; Falk-Petersen et al., 2001, Karnovsky et al., 2008).

Shelled pteropods of the genus *Limacina* (*L. helicina, L. retroversa*) also contribute significantly to vertical fluxes of both organic matter and biogenic calcium carbonate (Berner and Honjo, 1981; Bathmann et al., 1991; Hunt et al., 2008). Furthermore, thecosomes have a very thin and fragile shell made of aragonite, the more soluble form of calcium carbonate, and are the main planktonic producers of aragonite in the worlds' oceans (Lalli and Gilmer, 1989; Seibel et al., 2007). Due to the chemical structure of their shell, pteropods are expected to be among the first major group of calcifying organisms to be adversely effected by undersaturation in $CaCO_3$ (Orr et al., 2005; Seibel et al., 2007). Hence, due to its polar distribution, this will specifically apply to *Limacina helicina*.

In Svalbard waters *Limacina helicina* has a one-year life cycle. It develops to adults in early summer, and after reproduction in July/August their veligers grow to juveniles that overwinter until the next spring before development is completed (Gannefors et al., 2005; Lischka unpublished data). To cope with the high seasonality of food supply, many polar organisms reduce their metabolism to save energy and/or live on their energy reserves during winter (e.g. Hirche, 1996; Hagen and Auel, 2001; Lee et al., 2006). As for *L. helicina* it is not quite clear whether or not the species lowers its metabolism during overwintering and if so to what extent. Juveniles accumulate lipids and probably utilize them during the dark period (Gannefors et al., 2005). However, whatever the actual overwintering mode is, abiotic stressors will reduce species fitness

BGD
7, 8177–8214, 2010

with respect to survival. In other words, species resilience towards abiotic stress will be reduced during times of low energy supply and even more so, if metabolism is reduced as adaptation to winter conditions. Hence with respect to ocean acidification, *L. helicina* will have to withstand the most threatened period in a presumably vulnerable life stage and time.

Recently, the response to elevated pCO_2 partial pressures of adult *Limacina helicina* was investigated by Comeau et al. (2009, 2010b). In the later study, calcification was reduced as a function of pCO_2 at control and elevated temperature, whereas respiration was unaffected at control temperature but increased significantly as a function of pCO_2 at higher temperature. Hence, temperature can be a contributing factor to a species' response to changing pCO_2 partial pressures. In another investigation, he and co-workers studied larvae of the mediterranean species *Cavolinia inflexa* and reported on malformations, reduced shell growth and even shell-less, though still alive, larvae grown under low pH, respectively (Comeau et al., 2010a).

Furthermore, studies on pteropod shells collected in deep-sea sediment and traps provide evidence that shell integrity is lost with increasing degree of dissolution (Almogi-Labin et al., 1986; Acker and Byrne, 1989; Haddad and Droxler, 1996; Gerhardt et al., 2000; Manno et al., 2007). However, it is not possible from these findings to conclude on the effect of undersaturated waters on (the shell of) living pteropods. In fact, shell dissolution in live pteropods (*Clio pyramidata*) has so far only been described by Orr et al. (2005) by a coincidental observation.

The present investigation represents the first experimental study focusing on the combined effects of ocean acidification and elevated temperature on juveniles of the pteropod *Limacina helicina* from the Arctic Kongsfjord (Svalbard) prior to the overwintering period (mid September to end of October 2009). To study synergistic effects of elevated pCO_2 and temperature, incubation experiments were carried out at three different temperatures and four pCO_2 partial pressures to qualitatively assess the impact on species mortality, shell degradation, and shell growth. pCO_2 partial pressures chosen cover a range from pre-industrial values to levels forecasted to occur within this

BGD
7, 8177–8214, 2010

century (A2 scenariao, IPCC). The combination of three temperatures and four pCO_2 levels allow also to conclude on temperature and CO_2 effects separately.

2 Material and methods

2.1 Field sampling of pteropods

Juvenile *Limacina helicina* (Pteropoda, Thecosomata) were collected in Kongsfjord (northwest Spitsbergen) between 21 and 23 September 2009 using a plankton net (70 µm mesh size, 0.2 m^2 mouth opening, 1 l plastic cod end) onboard R/V Teisten (Kings Bay AS). Integrated vertical hauls were taken in the deepest accessible part of the fjord from 300 or 200 m depth to surface to allow collection of the deeper living overwintering individuals (Fig. 1). Onboard, freshly collected pteropods were stored in 20 l plastic containers in ambient seawater, and immediately transported to the Kings Bay Marine Laboratory where they were transferred into filtered seawater. In the laboratory, specimens were kept at in situ temperature (approx. 3 °C) in 1 µm filtered seawater until the start of experiments and for no longer than two days. Seawater supplied in the Marine Laboratory is pumped in 80 m depth from Kongsfjord and filtered through 20 µm filters. For experimental purpose it was additionally filtered through Whatman GF/B filters (approximately retaining particles larger than 1 µm). Furthermore, to characterize abiotic parameters, depth, temperature, and salinity were measured with a STD/CTD model SD-204 (manufactured by SAIV A/S, Bergen, Norway) prior to every sampling event.

2.2 Calcein staining

For qualitative assessment of shell growth under different temperature and pCO_2 conditions, pteropods were stained in a calcein bath (50 mg l^{-1}) for 1 h prior to incubation at experimental conditions. After staining, animals were rinsed with filtered seawater

BGD
7, 8177–8214, 2010

four times to remove excessive dye. Only actively moving individuals were taken for the experiments. Under UV-light, calcein has its fluorescence maximum at 515 nm (green) and marks the aperture margin at the time of staining (Comeau et al., 2009).

2.3 Experimental setup

In order to simulate past, present and future carbonate chemistries (atmospheric pCO_2 levels) (IPCC), GF/B filtered seawater was bubbled with air enriched with CO_2 using Wösthoff gas mixing pumps (Wösthoff, Germany) to levels of 180 µatm, 380 µatm, 750 µatm and 1150 µatm pCO_2 (target values) in storage containers at three temperatures (3, 5.5, and 8 °C). Six replicates were set up for each of the twelve. Prior to pipetting ten optically clean and actively moving juvenile *Limacina helicina* into each of the 440 ml jars (= one replicate), 5 ml filtered seawater were put in the jars to accommodate pteropods before filling the jars with the manipulated seawater. The whole procedure was done on crushed ice. After completion of all replicates of one temperature treatment (6 replicates X 4 pCO_2 levels = 24 glasses), jars were filled with the manipulated seawater at treatment temperature, closed with an air-tight lid and stored in a water bath in a climate room at the experimental temperature. Directly before filling experimental jars with manipulated seawater, water samples of each of the CO_2 manipulated seawater storage containers were taken (total alkalinity (A_T), nutrients) and pH on the total scale (pH_T) was measured. Nutrient samples were immediately deep-frozen (−20 °C) whereas A_T samples were poisoned with $HgCl_2$ and stored in a fridge subsequently (Dickson et al., 2007). After 29 days the experiment was terminated. Before harvesting juvenile *Limacina helicina*, pH_T was measured in each jar and water samples (A_T and nutrients) were taken. Subsequently, juveniles were collected from the jars and inspected for survival/mortality under a stereomicroscope and after rinsing in Milli-Q water, live (actively moving) individuals were preserved in 70% EtOH until inspection for shell degradation state and shell increment. Additionally, fjord water samples were taken for in situ A_T, dissolved inorganic carbon (C_T) and nutrient measurements.

BGD
7, 8177–8214, 2010

2.4 Analyses of the carbonate chemistry

pH on the total scale was calculated from voltage readings according to the guide of best practices for ocean CO_2 measurements (Dickson et al., 2007, SOP 6 a, 8.2). Instead of using TRIS buffers we used certified reference material (CRM) with a known pH calculated from known A_T and C_T (A. Dickson, Scripps Institution of Oceanography, La Jolla, California) as standard. Measurements were done using a pH Mobile 826 pH meter (Metrohm, Germany), precision was within 0.2 mV units.

Total alkalinity (A_T) was determined using a potentiometric titration device (Titrando 808, Metrohm) (Bradshaw et al., 1981). A_T was calculated from the Gran function as described by Dickson et al. (2003). The accuracy was determined by measuring CRM's as described for the pH measurements and precision was within 2 µmol kg^{-1}. For fjord water, dissolved inorganic carbon (C_T) was quantified with continuous-flow analysis (Bran & Luebbe QUAATRO photometer) according to Stoll et al. (2001). A_T accuracy was between 1 to 15 µmol kg^{-1}(differences between measured dicksons to target dickson, depending on prepared solutions and temperatures etc.) and C_T accuracy was between 40 to 50 µmol kg^{-1} (s.a.) Remaining carbonate system parameters for the experiments and fjord were calculated from A_T and pH, and A_T and C_T, respectively with the free software CO2SYS (Pierrot and Wallace 2006) using the constants from Mehrbach et al. (1973) refitted by Dickson and Millero (1987). Nutrients were analyzed according to Koroleff and Grasshof (1983).

CO_2 partial pressures at the start of the experiment differed slightly between replicates of the same CO_2 level, with consistently lower values at lower temperatures. We attribute this difference to temperature dependent equilibration rates, which increase with increasing temperature. Apparently three days of bubbling with CO_2/air gas mixtures were insufficient to achieve full equilibration of the medium.

BGD
7, 8177–8214, 2010

2.5 Mortality

After termination of the experiment, all juvenile *Limacina helicina* were inspected for survival under a stereomicroscope. For this, individuals were categorized optically into five different stages of activity (I = highest activity, V = no activity, or identified as dead)

Stage I: animal expanded, actively moving, soft tissue appears clear and in good condition

Stage II: animal retracted, actively moving inside shell, soft tissue appears clear and in good condition

Stage III: animal retracted, no discernable active movements, but soft tissue appears clear and in good condition, individual most likely alive

Stage IV: animal retracted, no discernable movements, soft tissue appears decomposed, individual most likely dead

Stage V: animal retracted, soft tissue appears strongly decomposed, individual clearly dead.

For statistical evaluation stages I–III (alive) and IV–V (dead) were pooled.

2.6 Shell degradation stage

Prior to shell degradation stage and shell growth (see below) analyses, soft tissue was removed with chlorine bleach.

BGD
7, 8177–8214, 2010

Shell integrity of all surviving individuals of all replicates was examined for surface degradation under a stereomicroscope (Leica MZ 16 F). Pteropod shells loose their integrity with increasing dissolution (e.g. Almogi-Labin et al., 1986; Gerhardt et al., 2000). Similar to Gerhardt et al. (2000), shell degradation was described qualitatively according to five categories, which are briefly described in the following (Fig. 2):

Category I: Shell transparency (applying oblique transmitted light) – shells were evaluated according to their transparency under oblique transmitted light. The scale extends from total transparency/clearness to different states of milky and cloudy shells, respectively.

Category II: Shell transparency (applying transmitted light) – using transmitted light, shells appear brownish to various extents.

Category III: Scarred structures – category III describes the frequency of scarred structures of any kind.

Category IV: Corrosion – category IV describes the deepness of scarred structures in the shell that can be estimated by focusing the stereomicroscope, hence category IV describes the severity of corrosion.

Category V: Perforation – in this category the number of holes in the shell is considered.

The condition of a single shell according to the different categories (except for category V) was described on a scale from 0–4 (in case of category V only 0–3). This leads to

BGD
7, 8177–8214, 2010

a maximum possible sum of 19 for shell degradation across all categories for a single shell. The maximum value was calculated for all inspected shells (Fig. 2), and for statistical analyses expressed as percentage of maximum possible surface degradation. In some cases, shells were mechanically damaged during processing. However, perforations due to corrosion can usually be distinguished from those resulting from mechanical damage. Therefore, only those perforations were counted in category V that securely could be identified as non-mechanical. Hence, shell surface degradation with respect to category V is underestimated.

Additionally, selected shells were examined by Scanning Electron Microscope (CamScan-CS-44, Institute of Geosciences, Kiel University) to illustrate shell degradation state specifically with respect to category IV and V more clearly and free of doubt, respectively (Fig. 3).

2.7 Analysis of shell growth

Shell growth deduced from calcein staining was measured on a Leica MZ 16 F stereomicroscope equipped with a UV-epifluorescence lamp and the Leica Application Suite 3.5.0. To standardize for individual size differences, not only the shell increment was measured but also the diameter, and the shell diameter and the ratio of shell increment to shell diameter were used for comparison between temperature treatments and CO_2 levels. One individual of each of the 6 replicates was analyzed (Fig. 4).

2.8 Statistics

Multifactorial analysis was performed to test for significant effects of the factors temperature and pCO_2 on mortality, shell degradation, shell diameter and the ratio of shell increment to shell diameter using a general linear model Type IV (GLM) for equal sample size in case of mortality and shell degradation and a GLM Type III model for unequal sample size in case of shell diameter and shell increment/diameter. Percentage data of mortality and shell degradation were Arcsin transformed, and values

BGD
7, 8177–8214, 2010

for the ratio shell increment/diameter were ˆ(λ-1)/ λ) transformed ($\lambda = 2.467508$, box-cox transformation). Data were tested for normality. In case of significant effects of temperature and/or pCO_2, homogeneity of variances was tested with Levene's test. To determine significant differences between temperature and pCO_2 treatments, respectively, a post-hoc Tukey's honest significant difference test (HSD and HSD for unequal n, respectively) with α-level 0.05 was used. Multiple regression analyses was performed to test whether or not shell degradation and shell growth under abiotic stress have an amplifying effect on mortality. All statistics were carried out using Statistica version 8 (Statsoft).

3 Results

3.1 Carbonate system

Carbonate chemistry conditions of the fjord were roughly simulated in the 380 µatm treatment as revealed by A_T, C_T and temperature (Table 1). Compared to in situ conditions the glacial treatment had an increased pH level and Ω_a whereas the CO_2 enriched treatments had diminished pH levels and subsaturated Ω_a conditions. At the end of the experiment, CO_2 partial pressures were higher compared to initial partial pressures. Accordingly pH and Ω_a levels were lower and pCO_2 was higher. Interestingly, also A_T values were slightly higher.

In the following, pCO_2 values (µatm) shown in figures are the means of values measured at experimental start.

3.2 Mortality

Temperature and pCO_2 both had a significant effect on mortality of *Limacina helicina* ($F = 60.055$, $p < 0.0001$ and $F = 5.831$, $p = 0.0009$, respectively). However, the temperature effect was stronger than the pCO_2 effect. There were no interactions between

BGD
7, 8177–8214, 2010

both factors ($F = 1.184$, $p = 0.32$, Table 2, significant values are in italics). Tukey HSD post-hoc test found mortality to be significantly higher at 5.5 °C and 8 °C ($p < 0.0001$ and $p < 0.0001$, respectively) as compared to in situ temperature (3 °C, Fig. 5a). Moreover, mortality was significantly higher at 8 °C as compared to 5.5 °C ($p = 0.03$). pCO_2 caused a significantly higher mortality at 1100 µatm as compared to 230 and 750 µatm ($p < 0.0001$ and $p = 0.03$, respectively, Fig. 5b), however, mortality at 1100 µatm did not significantly differ from 350 µatm ($p = 0.10$).

3.3 Shell degradation

Univariate test of significance revealed a significant effect of pCO_2 on shell degradation ($F = 118.969$, $p < 0.0001$). Temperature had no significant effect ($F = 2.060$, $p = 0.14$) and there were no interactions between factors ($F = 0.410$, $p = 0.87$, Table 3, significant values are in italics). Tukey HSD post-hoc test showed shell degradation did not differ between the lower pCO_2 treatments (230 and 350 µatm), but it was significantly less pronounced when compared to the 750 and 1100 µatm treatments. Furthermore, shell degradation was even more pronounced at 1100 µatm compared to 750 µatm (Fig. 6)

3.4 Shell growth

Univariate test of significance revealed a significant effect of pCO_2 on shell diameter ($F = 4.955$, $p = 0.003$) but not of temperature ($F = 1.767$, $p = 0.17$). Also, there were no interactions between the two factors ($F = 0.548$, $p = 0.76$, Table not shown). Tukey HSD post-hoc test revealed shell diameter of the high pCO_2 treatment (1100 µatm) to be significantly lower than the glacial (230 µatm) and the 750 µatm treatment, however, it was not significantly different from the 350 µatm treatment (Fig. 7).

Shell increment was significantly affected by pCO_2 ($F = 4.344$, $p = 0.008$), but neither by temperature ($F = 1.353$, $p = 0.27$) nor was an interactive effect between both factors found ($F = 2.044$, $p = 0.07$, Table 4, significant values are in italics). Tukey HSD post-hoc test revealed the shell increment/diameter ratio at the high pCO_2 treatment

BGD
7, 8177–8214, 2010

(1100 µatm) to be significantly lower than at 350 µatm and glacial CO_2 partial pressures, but not significantly different from the 750 µatm treatment (Fig. 8).

3.5 Effect of shell degradation and increment on mortality

Multiple regression analyses showed no significant amplifying effect of shell degradation and shell increment under abiotic stress on mortality (p for shell degradation and increment >0.44, Table 5). Also shell degradation and shell increment were not significantly correlated.

4 Discussion

The present experiments were carried out with unfed juvenile *Limacina helicina*. This approach is considered representative for the field situation since it seems unlikely that *L. helicina* juveniles were still actively feeding during the time of this investigation. Phytoplankton biomass decreases in Kongsfjorden already in late summer and fall (Hop et al., 2002), and phytoplankton abundance was extremely low during the whole period of investigation (own observations from a 20 µm net haul in the upper 20 m). Moreover, *L. helicina's* downward migration to overwintering depth (>100 m) begins in the first half of September in Kongsfjorden (Lischka, unpublished data) and the larger part of the population already dwelled between 100 to 200 m in mid September (as determined by stratified vertical net hauls). Hence, concerning food availability during the present study the conditions applied here resemble the natural situation of *L. helicina* not actively feeding anymore and presumably living on energy reserves (Gannefors et al., 2005) possibly, as we presume, at lower level metabolism.

4.1 Carbonate system

A_T at the end of the experiment showed a slightly increased trend with increasing temperature and pCO_2 that correlates with silicate concentrations. Most likely the A_T

BGD
7, 8177–8214, 2010

increase resulted from silicate and other components dissolved from the experimental jars.

Increased C_T concentrations and therefore decreased pH and Ω values as well as increased CO_2 partial pressures at the end are most likely explained by respiration of pteropods (and bacteria) in the closed experimental set up.

4.2 Effects of elevated temperature

Concerning mortality, temperature was the dominant factor as revealed by the higher F and lower p-value compared to those of pCO_2. This implies that juvenile *Limacina helicina* at the beginning of the overwintering phase are very sensitive to changes of 3 to 5 °C. Furthermore, multiple regression analysis showed that mortality is not significantly amplified by either of the other two effects (stage of shell degradation and shell growth). This is in contrast to Green et al. (2004, 2009) who point out that specifically dissolution was an important contributing factor to mortality of juvenile benthic bivalves that were exposed to aragonite undersaturation.

Limacina helicina is a north Atlantic subarctic species that is adapted to a relatively narrow and low temperature range between −0.4 °C and +4 °C and infrequently up to 7 °C (van der Spoel, 1967). As mentioned above, peak occurrence of *L. helicina* during the present investigation was between 100 and 200 m depth. In September/October 2009, a relatively warm water lens of about 5 to 5.5 °C occurred in Kongsfjorden between 40 and 110 m depth. Below 110 m, temperature decreased quickly to values below 4 °C down to a minimum of about 2 °C at 300 m. Furthermore, during the time of this investigation, *Limacina helicina* was at the onset of the overwintering period presumably not feeding anymore, likely living on lipid reserves. Temperature adaptation is a complex and energetically cost intensive metabolic response and costs of existence (the sum of all processes that are necessary to maintain viability, excluding reproduction, growth, and activity) vary significantly with temperature (Clarke, 2003). Hence, temperature stress during this period of *L. helicina's* life cycle can be a severe threat for its ability not only to survive the food-scarce winter period, but to survive

BGD
7, 8177–8214, 2010

with still enough energy reserves available to proceed development to adults and fuel reproduction in spring/summer.

4.3 Effects of elevated pCO_2

4.3.1 Shell increment and shell diameter

Similar to Reusch (1998), calcein was used here as a qualitative measure of shell growth. During our analyses it became evident, that calcein also serves as indicator for regions of enhanced calcifying activity. Strikingly, in juvenile *Limacina helicina* staining was not depicted as a distinct green line, but instead usually two main regions of coloration indicating calcification activity were observed. One region usually started with a distinct line on the outer whorl extending to the aperture (the actual shell increment), the other was found around the protoconch. This is in contrast to Comeau et al. (2009) who reported a distinct green line marking the shell edge (apertural margin) at the time of staining. The findings presented here are proposed as indication of "repair" calcification, since regions of coloration usually showed up where shell integrity was affected (Fig. 9). Indeed, thecosomes are able to repair shell parts (van der Spoel, 1967).

The question arising from this is why the region defined as shell increment was completely green instead of a single line marking the shell edge at time of staining and whether or not this region is indeed incremental or rather a region of enhanced shell thickening at the inner surface (presumably the inner prismatic layer, Sato-Okoshi et al., 2010)? In principle, concomitant shell diameter measurements on juveniles freshly caught in the field during the whole period of the experiment (data not shown) as well as the increasing shell diameters of the incubated individuals indicate growth of juvenile *Limacina helicina* during September/October 2009. To further address this question, dorso-lateral shell cross sections were made and revealed a fluorescence band at the inner shell surface, implying inward shell thickening (Fig. 10). However, close to the aperture, the whole shell cross section (that means according to Sato-Okoshi et

BGD
7, 8177–8214, 2010

al. (2010) the outer prismatic, middle crossed-lamellar, and inner prismatic layer) was fluorescent, thus implying shell increment. Therefore, the considered region is suggested as shell increment, where the proximal ("older") part of new increment is still thickened inwardly (inner prismatic layer), and close to the apertural margin true shell increment proceeds. A similar process is described for the pteropod *Cuvierina columnella* (Cavoliniidae), which after attaining maximum shell length continues to thicken the entire shell inwardly (Lalli and Gilmer, 1989). Moreover, if our hypothesis is true for *L. helicina*, the fact that the entire region of increment was green points to storage of calcein during the entire incubation time.

Shell growth of *Limacina helicina* kept at 1100 µatm was significantly reduced as compared to individuals kept at the 350 and 230 µatm. However, *L. helicina* was able to grow at $\Omega_a < 1$. In that, the present results principally agree with the conclusion by Comeau et al. (2009) deduced from adult *L. helicina* that seemed to be well adapted to aragonite undersaturation. However, in addition to shell growth, shell degradation state of juvenile *L. helicina* revealed pronounced dissolution processes at the same time and as mentioned earlier, "repair" calcification is suggested. Therefore, two crucial questions arise: (1) How well can juvenile *L. helicina* adapt to aragonite undersaturation and what are the costs for different life stages of *L. helicina* to afford growth/calcification and prevent dissolution under aragonite undersaturation? (2) Will it be possible for *L. helicina* at the same time to sustain development, reproduction and accumulation of energy reserves to overwinter? The intensity of shell degradation under the two high pCO_2 levels leads to the conclusion that juvenile pre-winter *L. helicina* may be seriously threatened under aragonite undersaturation.

The present study shows that pCO_2 is the driving factor influencing shell growth and calcification, whereas temperature had no significant influence. This is in agreement with recent findings for adult *Limacina helicina* that exhibited declined precipitation rates of $CaCO_3$ as a function of pCO_2 (Comeau et al., 2010b).

BGD
7, 8177–8214, 2010

4.3.2 Shell degradation

Both elevated pCO_2 levels caused a significant effect on shell degradation, and furthermore, shell degradation was more pronounced at 1100 µatm as compared to 750 µatm. Hence, shell degradation state gives clear evidence that juvenile *Limacina helicina* are negatively affected by aragonite saturation levels below 1. To the authors knowledge dissolution in live pteropods has so far only been reported by Orr et al. (2005) and Comeau at el. (2010a) from a North Atlantic and a Mediterranean species, respectively (*Clio pyramidata* and *Cavolinia inflexa*). Similar to the present results, shell surface alterations due to $CaCO_3$ undersaturation are reported by e.g. Green et al. (2009) on live juvenile benthic bivalves, and from *Limacina* spp. shells collected in sediment traps by Gerhardt et al. (2000) and Manno et al. (2007).

Although only pCO_2 significantly affected shell integrity, the results suggest temperature to also have some influence. If shell degradation data was plotted against temperature a negative trend with increasing temperatures across all pCO_2 treatments is observed. Additionally most perforations were found in shells from individuals that were incubated at in situ temperature and high pCO_2 compared to less shells with perforations in the high temperature/high pCO_2 treatment. However, in the latter case more counts in category IV (corrosion) as compared to counts in category V (perforations) led to an equally high maximum sum for shell degradation. Hence, at higher temperature and presumably due to a higher metabolism (Q_{10}), *L. helicina* might be better able to counteract dissolution processes by 'repair' calcification and by that being able to avoid perforation at least for a limited time. Similar to this, McDonald et al. (2009) describe compensatory calcification in the intertidal barnacle *Amphibalanus amphitrite* that was exposed to acidified conditions and showed compensatory calcification of their basal shell plates but central shell wall plates were significantly weakened.

BGD
7, 8177–8214, 2010

5 Conclusions

The findings shown here give insight to the response character (mortality, shell degradation, shell increment) and plasticity of juvenile *Limacina helicina* in preparation for overwintering as a function of temperature and pCO_2. Increasing temperature and pCO_2 act differently on *L. helicina*, both significantly increasing species mortality and only the latter significantly affecting shell integrity and shell growth. pCO_2 changes as projected in scenarios for the near future may severely affect pre-winter juveniles, and rising temperatures could contribute to a decline in abundance of the overwintering population, which represents the basis for next year's reproduction. Hence, population dynamics are likely to be changed and consequences for the Arctic epipelagic ecosystem may arise.

Various questions arise from this study with respect to *Limacina helicina's* fate in a high CO_2 ocean. Higher metabolic activity is proposed to compensate for dissolution and higher metabolic costs as possible reason for higher mortality of *L. helicina* at higher temperature. This raises the question as to energetic costs/trade offs and to what extent compensatory metabolic costs can be tolerated without seriously threatening winter survival and ultimately reproductive success? To address these questions, further detailed studies on the response to rising CO_2 partial pressures and temperature and in due consideration of *L. helicina's* life stages and life cycle including physiological investigations (e.g. respiration, lipid utilization) are needed.

Acknowledgements. We thank the staffs of the AWIPEV Station of the Alfred-Wegener-Institute for Polar and Marine Research and Kings Bay AS in Ny-Ålesund for excellent logistical support during our field campaign. The Institute for Polar Ecology in Kiel is acknowledged for making logistics and optical facilities available to us. The scanning electron microscopy work was done in the Institute of Geosciences in Kiel, particularly we are indebted to Ute Schuldt for her supervision in the SEM Lab. Thanks are also due to Armin Form for helpful discussions, as well as Mark Lenz and Dieter Piepenburg for statistical advice. This work is a contribution to the German BMBF (Federal Ministry of Education and Research) funded project "Biological Impacts of Ocean Acidification" (BIOACID, Grant number 03F0608A). This work also received

BGD
7, 8177–8214, 2010

funding from the European Centre for Arctic Environmental Research (ARCFAC, Grant number 026129-2008-54).

References

Acker, J. G. and Byrne, R. H.: The influence of surface state and saturation state on the dissolution kinetics of biogenic aragonite in seawater, Am. J. Sci., 289, 1098–1116, 1989.

Almogi-Labin, A., Luz, B., and Duplessy, J.-C.: Quaternary paleo-oceanography, pteropod preservation and stable-isotope record of the Red Sea, Paleogr. Paleoclimatol. Paleoecol., 57, 195–211, 1986.

Bathmann, U. V., Noji, T. T., and von Bodungen, B.: Sedimentation of pteropods in the Norwegian Sea in autumn, Deep-Sea Res., 38, 1341–1360, 1991.

Berner, R. A. and Honjo, S.: Pelagic sedimentation of aragonite: its geochemical significance, Science, 211, 940–942, 1981.

Bradshaw, A. L., Brewer, P. G., Shafer, D. K., and Williams, R. T.: Measurements of total carbon dioxide and alkalinity by potentiometric titration in the GEOSECS program, Earth Planet Sci. Lett., 55, 99–115, 1981.

Clark, D., Lamare, M., and Barker, M.: Response of sea urchin pluteus larvae (Echinodermata: Echinoidea) to reduced seawater pH: a comparison among a tropical, temperate, and a polar species, Mar. Biol., 156, 1125–1137, 2009.

Clarke, A.: Costs and consequences of evolutionary temperature adaptation. Trends Ecol. Evol., 18, 573–581, 2003.

Comeau, S., Gorsky, G., Jeffree, R., Teyssié, J. L., and Gattuso, J. P.: Impact of ocean acidification on a key Arctic pelagic mollusc (*Limacina helicina*), Biogeosciences, 6, 1877–1882, 2009, http://www.biogeosciences.net/6/1877/2009/.

Comeau, S., Gorsky, G., Alliouane, S., and Gattuso, J. P.: Larvae of the pteropod *Cavolinia inflexa* exposed to aragonite undersaturation are viable but shell-less, Mar. Biol. 157, 2341–2345, 2010a.

Comeau, S., Jeffree. R., Teyssié, J. L., and Gattuso, J. P.: Response of the Arctic Pteropod *Limacina helicina* to Projected Future Environmental Conditions PLoS ONe, 5(6), e11362, 2010b.

BGD

7, 8177–8214, 2010

Dickson, A. G. and Millero, F. J.: A comparison of the equilibrium constants for the dissociation of carbonic acid in seawater media, Deep-Sea Res Pt. A, 34, 1733–1743, 1987.
Dickson, A. G., Afghan, J. D., and Anderson, G. C.: Reference materials for oceanic CO_2 analysis: a method for the certification of total alkalinity, Mar. Chem., 80, 185–197, 2003.
Dickson, A. G., Sabine, C. L., and Christian, J. R.: Guide to the best practices for ocean CO_2 measurements, PICES Special Publication, 3, 191 pp., 2007.
Fabry, V. J., Seibel, B. A., Feely, R. A., and Orr, J. C.: Impacts of ocean acidification on marine fauna and ecosystem processes, ICES J. Mar. Sci., 65, 414–432, 2008.
Falk-Petersen, S., Sargent, J. R., Kwasniewski, S., Gulliksen, B., and Millar, R. M.: Lipids and fatty acids in *Clione limacina* and *Limacina helicina* in Svalbard waters and the Arctic Ocean: trophic implications, Polar Biol., 24, 163–170, 2001.
Gannefors, C., Böer, M., Kattner, G., Graeve, G., Eiane, K., Gulliksen, B., Hop, H., and Falk-Petersen, S.: The Arctic sea butterfly *Limacina helicina*: lipids and life strategy, Mar. Biol., 147, 169–177, 2005.
Gazeau, F., Quiblier, C., Jansen, J. M., Gattuso, J.-P., Middelburg, J. J., and Heip, C. H. R.: Impact of elevated CO_2 on shellfish calcification, Geophys. Res. Lett., 34, L07603, doi:10.1029/2006GL028554, 2007.
Gerhardt, S., Groth, H., Ruehlemann, C., and Henrich, R.: Aragonite preservation in late Quaternary sediment cores on the Brazilian Continental Slope: implications for intermediate water circulation, Int. J. Earth Sci., 88, 607–618, 2000.
Gilmer, R. W. and Harbison, G. R.: Diet of *Limacina helicina* (Gastropoda: Thecosomata) in Arctic waters in midsummer, Mar. Ecol. Prog. Ser., 77, 125–134, 1991.
Green, M. A., Jones, M. E., Boudreau, C. L., Moore, R. L., and Westman, B. A.: Dissolution mortality of juvenile bivalves in coastal marine deposits, Limnol. Oceanogr., 49, 727–734, 2004.
Green, M. A., Waldbusser, G. G., Reilly, S. L., Emerson, K., and O'Donnell, S.: Death by dissolution: Sediment saturation state as a mortality factor for juvenile bivalves, Limnol. Oceanogr., 54, 1048–1059, 2009.
Guinotte, J. M. and Fabry, V. J.: Ocean Acidification and Its Potential Effects on Marine Ecosystems, Ann. NY Acad. Sci., 1134, 320–342, 2008.
Gutowska, M. A., Melzner, F., Pörtner, H. O., and Meier, S.: Cuttlebone calcification increases during exposure to elevated seawater pCO_2 in the cephalopod *Sepia officinalis*, Mar. Biol., 157, 1653–1663, 2010.

BGD
7, 8177–8214, 2010

Haddad, G. A. and Droxler, A. W.: Metastable $CaCO_3$ dissolution at intermediate water depths of the Caribbean and western North Atlantic: Implications for intermediate water circulation during the past 200 000 years, Paleoceanography, 11, 701–716, 1996.
Hagen, W. and Auel, H.: Seasonal adaptations and the role of lipids in oceanic zooplankton, Zoology, 104, 313–326, 2001.
Hirche, H.-J.: Diapause in the marine copepod, *Calanus finmarchicus* – a review, Ophelia, 44, 129–143, 1996.
Hop, H., Pearson, T., Hegseth, E. N., Kovacs, K. M., Wiencke, C., Kwasniewski, S., Eiane, K., Mehlum, F., Gulliksen, B., Wlodarska-Kowalczuk, M., Lydersen, C., Weslawski, J. M., Cochrane, S., Gabrielsen, G. W., Leakey, R. J. G., Lønne, O. J., Zajaczkowski, M., Falk-Petersen, S., Kendall, M., Wängberg, S.-Å., Bischof, K., Voronkov, A. Y., Kovaltchouk, N. A., Wiktor, J., Poltermann, M., di Prisco, G., Papucci, C., and Gerland, S.: The marine ecosystem of Kongsfjorden, Svalbard, Polar Res., 21, 167–208, 2002.
Hunt, B. P. V., Pakhomov, E. A., Hosie, G. W., Siegel, V., Ward, P., and Bernard, K.: Pteropods in Southern Ocean ecosystems, Prog. Oceanogr., 78, 193–221, 2008.
Karnovsky, N. J., Hobson, K. A., Iverson, S., and Hunt, G. L.: Seasonal changes in diets of seabirds in the North Water Polynya: a multiple-indicator approach, Mar. Ecol. Prog. Ser., 357, 291–299, 2008.
Koroleff, F. and Grasshoff, K.: Determination of nutrients, in: Methods of seawater analysis, edited by: Grasshoff, K., Ehrhardt, M., Kremling, K., Verlag Chemie, Weinheim, 419 pp., 1983.
Kurihara, H.: Effects of CO_2-driven ocean acidification on the early developmental stages of invertebrates, Mar. Ecol. Prog. Ser., 373, 275–284, 2008.
Kurihara, H., Kato, S., and Ishimatsu, A.: Effects of increased seawater pCO_2 on early development of the oyster *Crassostrea gigas*, Aquat. Biol., 1, 91–98, 2007.
Lalli, C. M. and Gilmer, R. W.: Pelagic snails: the biology of holoplanktonic gastropod molluscs, Stanford University Press, 259 pp., 1989.
Lee, R. F., Hagen, W., and Kattner, G.: Lipid storage in marine zooplankton, Mar. Ecol. Prog. Ser., 307, 273–306, 2006.
Manno, C., Sandrini, S., Tositti, L., and Accornero, A.: First stages of degradation of *Limacina helicina* shells observed above the aragonite chemical lysocline in Terra Nova Bay (Antarctica), J. Mar. Syst., 68, 91–102, 2007.
McDonald, M. R., McClintock, J. B., Amsler, C. D., Rittschof, D., Angus, R. A., Orihuela, B., and

BGD
7, 8177–8214, 2010

Lutostanski, K.: Effects of ocean acidification over the life history of the barnacle *Amphibalanus amphitrite*, Mar. Ecol. Prog. Ser., 385, 179–187, 2009.
Mehrbach, C., Culberson, C. H., Hawley, J. E., and Pytkowicz, R. M.: Measurement of the apparent dissociation constants of carbonic acid in seawater at atmospheric pressure, Limnol. Oceanogr., 18, 897–907, 1973.
Orr, J. C., Fabry, V. J., Aumont, O., Bopp, L., Doney, S. C., Feely, R. A., Gnanadesikan, A., Gruber, N., Ishida, A., Joos, F., Key, R. M., Lindsay, K., Maier-Reimer, E., Matear, R., Monfray, P., Mouchet, A., Najjar, R. G., Plattner, G.-K., Rodgers, K. B., Sabine, C. L., Sarmiento, J. L., Schlitzer, R., Slater, R. D., Totterdell, I. J., Weirig, M.-F., Yamanaka, Y., and Yool, A.: Anthropogenic ocean acidification over the twenty-first century and its impact on calcifying organisms, Nature, 437, 681–686, 2005.
Pierrot, D. E. L. and Wallace, D. W. R.: MS Excel program developed for CO2 System Calculations. ORNL/CDIAC-105, Oak Ridge, Tennessee, Carbon Dioxide Information Analysis Center, Oak Ridge National Laboratory, U.S. Department of Energy, 2006.
Reusch, T. B. H.: Differing effects of eelgrass *Zostera marina* on recruitment and growth of associated blue mussels *Mytilus edulis*, Mar. Ecol. Prog. Ser., 167, 149–153, 1998.
Riebesell, U., Zondervan, I., Rost, B., Tortell, P. D., Zeebe, R. E., and Morel, F. M. M.: Reduced calcification of marine plankton in response to increased atmospheric CO_2, Nature, 407, 364–367, 2000.
Sato-Okoshi, W., Okoshi, K., Sasaki, H., and Fumihiro, A.: Shell structure of two polar pelagic molluscs, Arctic *Limacina helicina* and Antarctic *Limacina helicina antarctica* forma antarctica, Polar Biol., doi:10.1007/s00300-010-0849-1, 2010.
Seibel, B. A., Dymowska, A., and Rosenthal, J.: Metabolic temperature compensation and coevolution of locomotory performance in pteropod molluscs, Integr. Comp. Biol., 47, 880–891, 2007.
Spoel, van der S. V. D.: Euthecosomata a group with remarkable developmental stages (Gastropoda, Pteropoda), Zoological Museum, Amsterdam, 375 pp., 1967.
Steinacher, M., Joos, F., Frlicher, T. L., Plattner, G.-K., and Doney, S. C.: Imminent ocean acidification in the Arctic projected with the NCAR global coupled carbon cycle-climate model, Biogeosciences, 6, 515–533, doi:10.5194/bg-6-515-2009, 2009.
Stoll, M. H. C., Bakker, K., Nobbe, G. H., and Haese, R. R.: Continuous-Flow Analysis of Dissolved Inorganic Carbon Content in Seawater, Anal. Chem., 73, 4111–4116, 2001.
Wilson, J. G.: Environment and birth defects, Academic, New York, 305 pp., 1973.

BGD
7, 8177–8214, 2010

Table 1. Mean carbonate system parameters calculated from samples taken from the prepared manipulated seawater at start and from all experimental jars at the end of the experimental period. The treatment column refers to target temperature and pCO_2, of which the pCO_2 levels refer to glacial partial pressure CO_2 (180 µatm, 18 kyr BC), present day pCO_2 (380 µatm, year 1990), high pCO_2 I (750 µatm, year 2080), and high pCO_2 II (1150 µatm, > year 2100). The concentration of total CO_2 (C_T), partial pressure of CO_2 (pCO_2), and the saturation state of aragonite (Ω_a) were derived from pH_T, total alkalinity (A_T), salinity (Sal) and temperature (T). Si is silicate.

Treatment		Sal	T (°C)		A_T (µmol kg^{-1})		pH_T		C_T (µmol kg^{-1})		pCO_2 (µatm)		Ω_a		Si (µmol kg^{-1})	
Temp (°C)	ppm		start	end	start	end	start	end	start	end	start	end	start	end	start	end
3	180	34.7	3.5	3.6	2280	2288	8.27	8.28	2045	2047	216	211	2.45	2.51	2.63	6.49
	380	34.7	3.3	3.5	2280	2287	8.12	8	2115	2164	323	435	1.81	1.45	2.63	7.27
	750	34.7	3.1	3.6	2280	2291	7.81	7.78	2223	2241	703	764	0.95	0.91	2.63	11.82
	1150	34.7	3	3.5	2280	2296	7.69	7.62	2260	2291	948	1110	0.72	0.65	2.63	11.25
5.5	180	34.7	5.4	5.4	2280	2288	8.24	8.09	2041	2118	231	347	2.5	1.87	2.63	3.47
	380	34.7	5.5	5.4	2280	2295	8.09	8.03	2111	2150	348	411	1.86	1.65	2.63	8.91
	750	34.7	5.6	5.4	2280	2293	7.8	7.74	2215	2246	732	851	1.02	0.9	2.63	4.38
	1150	34.7	5.6	5.4	2280	2299	7.66	7.63	2256	2283	1026	1104	0.76	0.71	2.63	12.28
8	180	34.7	8	7.6	2280	2290	8.26	8.12	2012	2092	223	322	2.8	2.15	2.63	7.3
	380	34.7	7.9	7.6	2280	2293	8.11	8	2086	2146	333	445	2.11	1.68	2.63	15.22
	750	34.7	7.9	7.5	2280	2302	7.81	7.73	2199	2247	711	876	1.15	0.96	2.63	16.18
	1150	34.7	8.1	7.5	2280	2305	7.62	7.58	2256	2297	1138	1279	0.77	0.69	2.63	16.46
Fjord (200 m)		35	3.9	4.3	2296	2287	7.98	8.03	2174	2145	448	398	1.45	1.61	3.27	3.13

BGD
7, 8177–8214, 2010

Table 2. Univariate tests of significance indicating the effect of temperature and pCO_2 on mortality.

Effect	SS	df	MS	*F*	*p*
Intercept	84.734	1	84.734	1362.562	0.000
Temp.	7.469	2	3.735	60.055	*0.000*
pCO_2	1.088	3	0.363	5.831	*0.0009*
Temp. x pCO_2	0.442	6	0.074	1.184	0.32
Error	8.209	132	0.062		

BGD
7, 8177–8214, 2010

Table 3. Univariate tests of significance indicating the effect of pCO_2 on shell degradation.

	SS	df	MS	*F*	*p*
Intercept	21.402	1	21.402	3143.201	0.000
Temp.	0.028	2	0.014	2.060	0.14
pCO_2	2.430	3	0.810	118.969	*0.000*
Temp. x pCO_2	0.017	6	0.003	0.410	0.87
Error	0.409	60	0.007		

BGD
7, 8177–8214, 2010

Table 4. Univariate tests of significance indicating the effect of pCO_2 on the ratio of shell increment to shell diameter.

	SS	df	MS	*F*	*p*
Intercept	34.772	1	34.772	4249.554	0.000
Temp.	0.022	2	0.011	1.353	0.27
pCO_2	0.107	3	0.036	4.344	*0.008*
Temp. x pCO_2	0.100	6	0.017	2.044	0.07
Error	0.507	62	0.008		

BGD
7, 8177–8214, 2010

Table 5. Univariate tests of significance indicating the effect of shell degradation and shell increment on mortality

Effect	SS	df	MS	*F*	*p*
Intercept	2.414212	1	2.414	18.053	0.000
Shell degradation	0.079527	1	0.080	0.595	0.443
Shell increment	0.056430	1	0.056	0.422	0.518
Error	8.692226	65	0.134		

BGD
7, 8177–8214, 2010

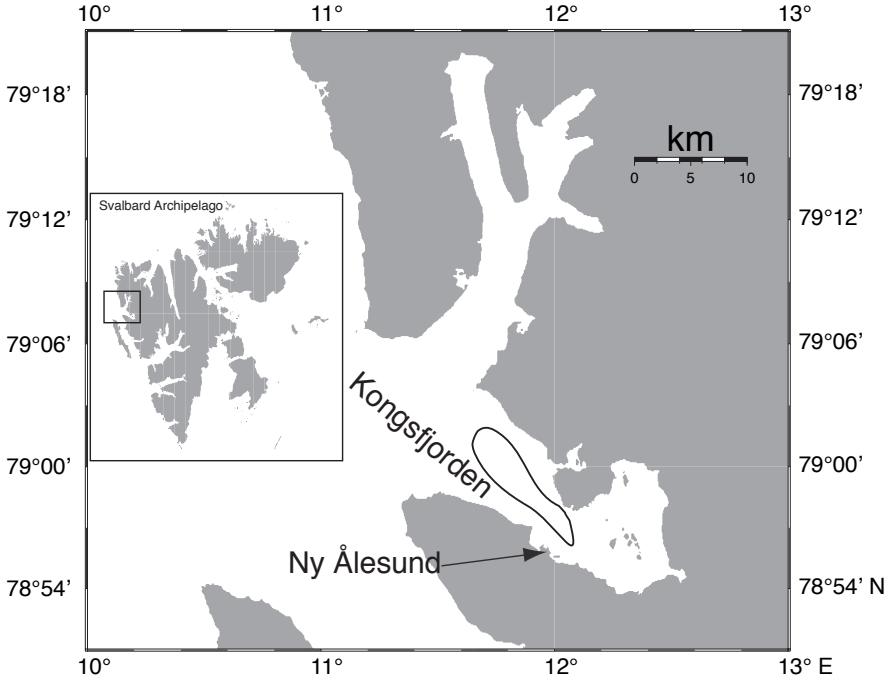

Fig. 1. Map of Kongsford with sampling area.

BGD
7, 8177–8214, 2010

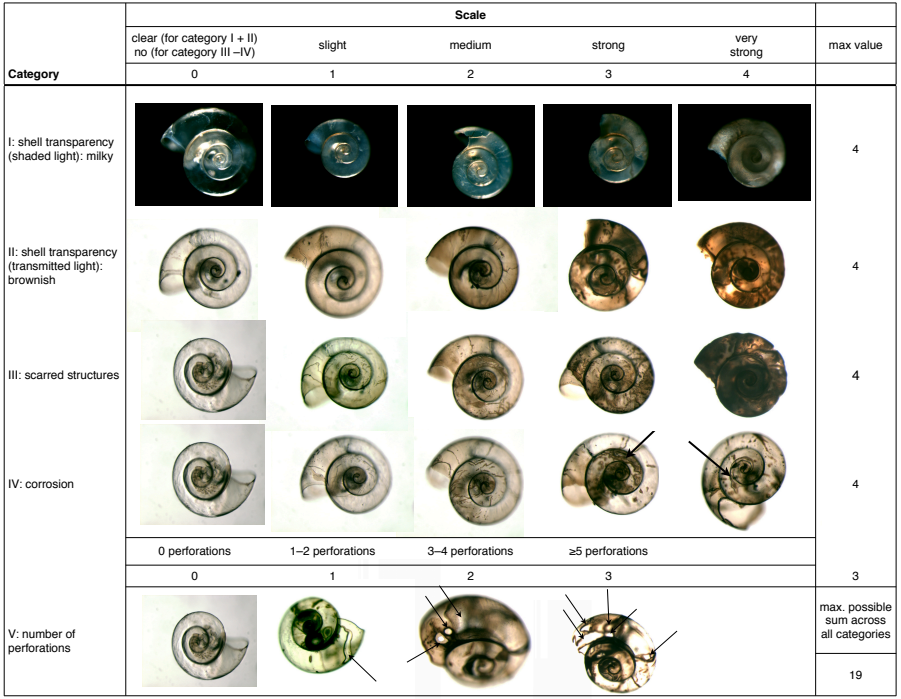

Fig. 2. Categories of shell degradation (I–V) and their levels of conspicuities on a scale from 0–4 (for category I–IV) and 0–3 (for category V), respectively. See also Fig. 3 for category IV and V.

BGD
7, 8177–8214, 2010

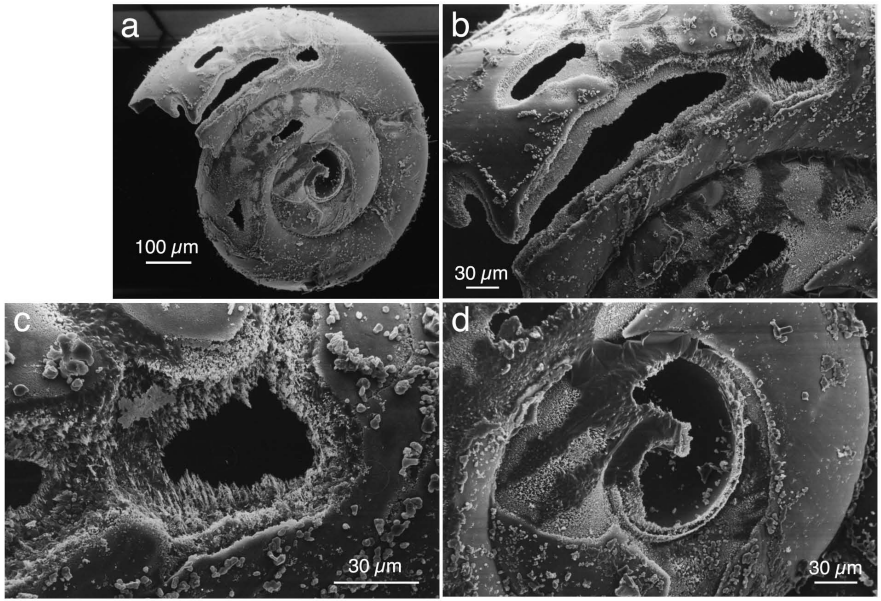

Fig. 3. Scanning electron micrographs (SEM) of representative *Limacina helicina* reared at 3 °C/1100 µatm to illustrate shell degradation state specifically with respect to category IV and V more clearly and free of doubt, respectively. Magnification and scale bars are shown. Individual shown here is the same as shown in Fig. 2 for category V with ≥5 perforations.

BGD
7, 8177–8214, 2010

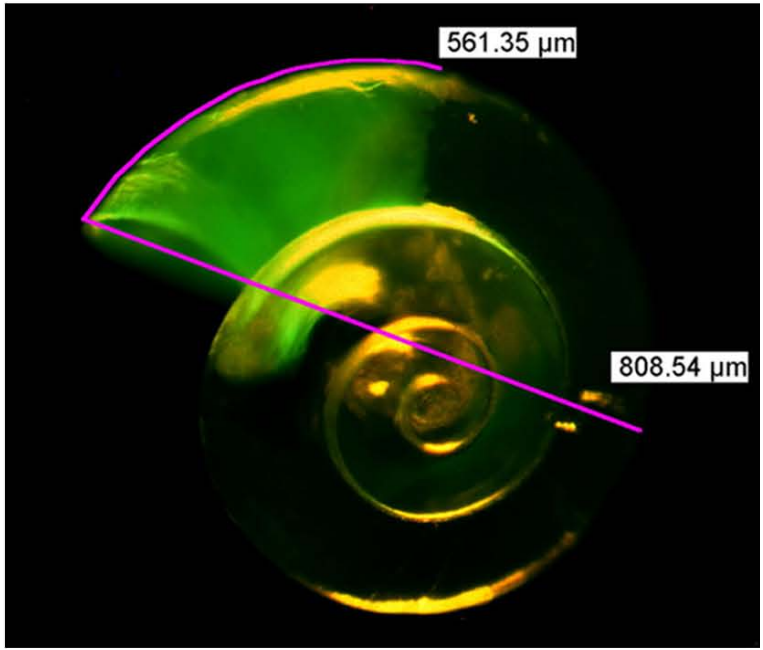

Fig. 4. Calcein stained shell of *Limacina helicina* showing shell increment during experiment and measurement of increment length and diameter.

BGD
7, 8177–8214, 2010

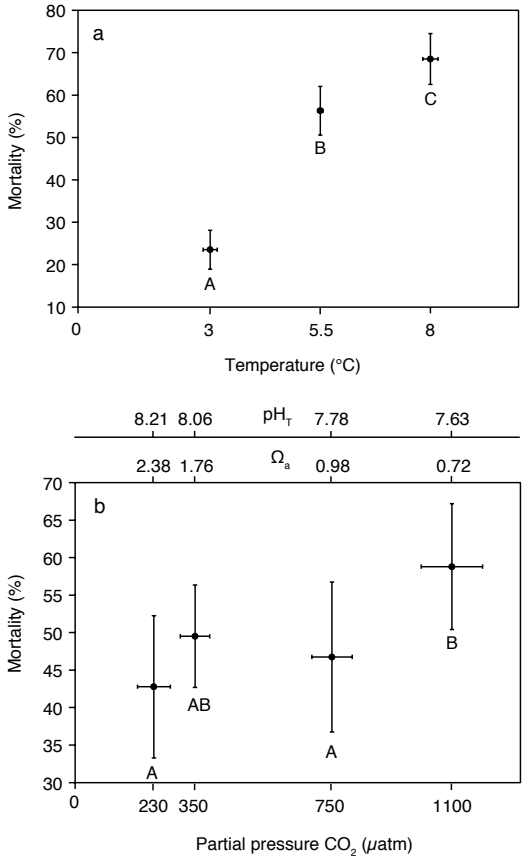

Fig. 5. % mortality after 29 days of incubation of *Limacina helicina*. Means for the effects of **(a)** temperature and **(b)** pCO_2. Vertical bars denote 0.95 confidence intervals for mortality, horizontal bars denote 0.95 confidence intervals for pCO_2. Results from the Tukey HSD post-hoc test are depicted by letters with levels not connected by same letter being significantly different.

BGD
7, 8177–8214, 2010

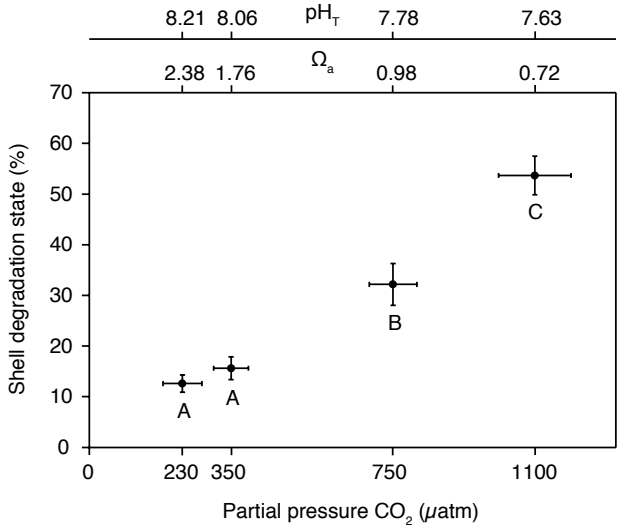

Fig. 6. % value for shell degradation after 29 days of incubation of *Limacina helicina*. Mean for the effect of pCO_2. Vertical bars denote 0.95 confidence intervals for shell degradation, horizontal bars denote 0.95 confidence intervals for pCO_2. Results from the Tukey HSD post-hoc test are depicted by letters with levels not connected by same letter being significantly different.

BGD
7, 8177–8214, 2010

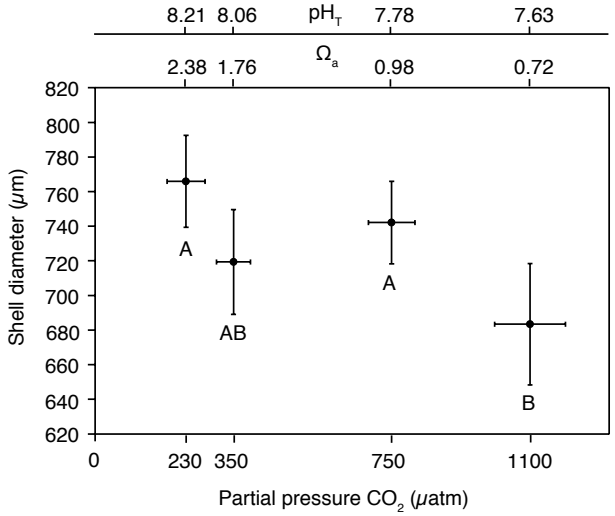

Fig. 7. Mean diameter of *Limacina helicina* after 29 days of incubation for the effect of pCO_2. Vertical bars denote 0.95 confidence intervals for diameter, horizontal bars denote 0.95 confidence intervals for pCO_2. Results from the Tukey HSD post-hoc test are depicted by letters with levels not connected by same letter being significantly different.

BGD
7, 8177–8214, 2010

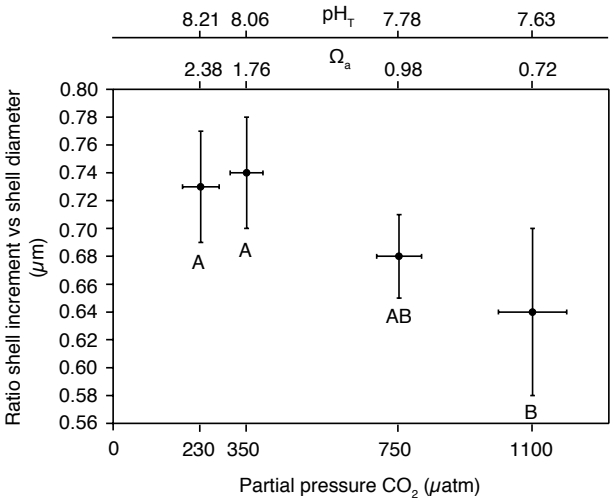

Fig. 8. Mean shell increment per diameter ratio of *Limacina helicina* after 29 days of incubation for the effect of pCO_2. Vertical bars denote 0.95 confidence intervals for mean shell increment/diameter, horizontal bars denote 0.95 confidence intervals for pCO_2. Results from the Tukey HSD post-hoc test are depicted by letters with levels not connected by same letter being significantly different.

BGD
7, 8177–8214, 2010

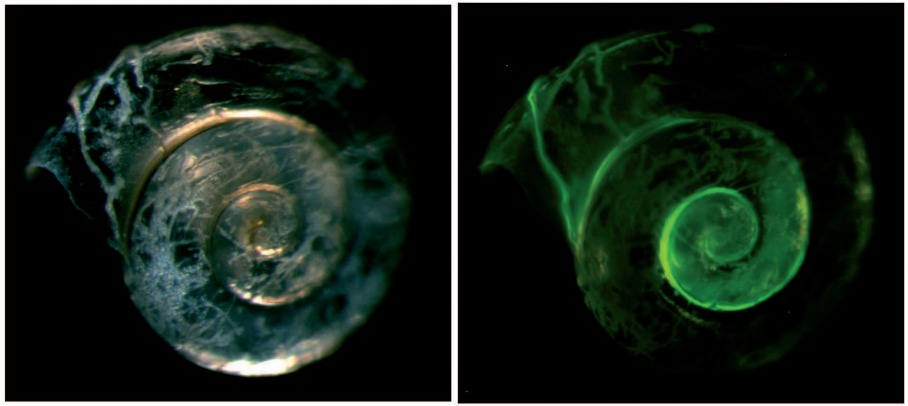

Fig. 9. Example for “repair” calcification: shell degradation of *Limacina helicina* (right, opaque transmitted light) and the respective regions of “repair” calcification indicated by enhanced fluorescence due to calcein incorporation (left).

BGD
7, 8177–8214, 2010

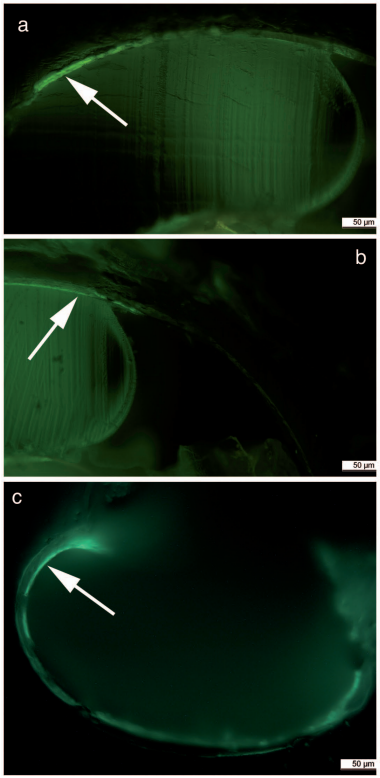

Fig. 10. Cross sections of *Limacina helicina* shells in the region of shell increment. **(a)** Dorso-lateral section showing calcein incorporation in all shell layers (prismatic, middle crossed-lamellar, inner prismatic) close to the aperture (arrow). **(b)** Higher magnification of the right part of (a) with arrow pointing at the thin inner fluorescence line. **(c)** Cross section of the aperture region distal from the area of increment, the arrow pointing at the line of constructive processes at the inner prismatic shell layer. All photos were taken using a Leica Aristoplan epifluourescence microscope.

BGD
7, 8177–8214, 2010